

# Design and synthesis of novel 2-methyl-4,5-substitutedbenzo[f]-3,3a,4,5-tetrahydro-pyrazolo[1,5-d][1,4]oxazepin-8(7H)-one derivatives as telomerase inhibitors

Xin-Hua Liu<sup>a,b,\*</sup>, Ying-Ming Jia<sup>c</sup>, Bao-An Song<sup>a</sup>, Zhi-xiang Pang<sup>b</sup>, Song Yang<sup>a,\*</sup>

<sup>a</sup> Key Laboratory of Green Pesticide and Agriculture Bioengineering, Ministry of Education, Guizhou University, Guiyang 550025, PR China

<sup>b</sup> School of Pharmacy, Anhui Medical University, Hefei 230032, PR China

<sup>c</sup> School of Chemistry and Chemical Engineering, Anhui University of Technology, Maanshan 243002, PR China

## ARTICLE INFO

### Article history:

Received 11 September 2012

Revised 19 November 2012

Accepted 22 November 2012

Available online 3 December 2012

### Keywords:

Synthesis

Hydropyrazolo-oxazepine

PI3K/AKT pathway

Antitumor agents

## ABSTRACT

Eight novel 4,5-tetrahydropyrazolo[1,5-d][1,4]oxazepine derivatives have been synthesized and purified to be screened for anticancer activity. By a modified TRAP assay, some titled compounds were tested against telomerase, and compound **4a** showed the most potent inhibitory activity with IC<sub>50</sub> value at 0.78 ± 0.22 μM. Western blot assays showed that compounds **4a** and **4b** could inhibit expression of Cyclin D1, TERT, phospho-AKT and PI3K/AKT pathway.

© 2012 Elsevier Ltd. All rights reserved.

Telomerase represents one of the promising targets in drug discovery.<sup>1–4</sup> Human telomerase reverse transcriptase is a catalytic enzyme that is required for cancer progression.<sup>5</sup> Recent studies indicate that the PI3K/AKT pathway is targeted by amplification, mutation and translocation more frequently than any other pathway in cancer patients.<sup>6</sup>

Heterocyclic seven-membered ring constitute the core or a key fragment of a number of bioactive compounds including isolated from natural products.<sup>7–9</sup> Among them, seven-membered heterocycles with two heteroatoms in 1,4-distance are known to possess manifold biological activity. In particular, [1,4]oxazepine units are crucial moieties in several psychoactive pharmaceuticals (for example, oxazepam), among a variety of physiologically active 1,4-oxazepines, the derivatives of their aryl-fused analogs represent a relatively little-explored group with interesting pharmaceutical properties. They were described as effective protease inhibitors, non-peptidergic GPCR inhibitors, integrin antagonists, squalene synthase, and reverse transcriptase inhibitors.<sup>10–12</sup>

**Abbreviations:** PI3K, phosphatidylinositol 3-kinase; AKT, serine/threonine Kinase; GPCR, G-protein coupled receptor; hTERT, human telomerase reverse transcriptase subunit; BIBR1532, 2-[E]-3-naphthalen-2-yl-but-2-enylamino]-benzoic acid; MGC-803, The human gastric carcinoma cell line.

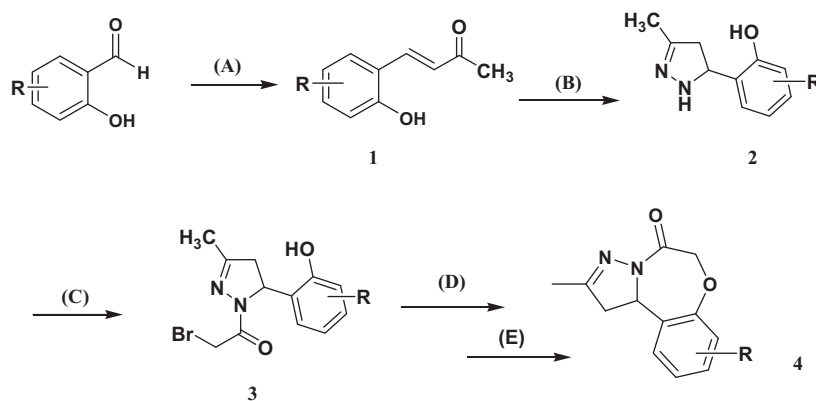
\* Corresponding author. Tel.: +86 851 3161115; fax: +86 851 3620521.

E-mail addresses: [xhliuhx@163.com](mailto:xhliuhx@163.com) (X.-H. Liu), [yangsdqj@126.com](mailto:yangsdqj@126.com) (S. Yang).

Many 3,4-dihydropyrazole-based derivatives have shown several biological activities as seen in cannabinoid receptor 1 antagonist, monoamine oxidase inhibitors, and tumor necrosis inhibitors.<sup>13</sup> In our recent publications, several ary-dihydropyrazole derivatives used as potent telomerase inhibitors were described.<sup>14,15</sup>

In an effort to design novel ary-dihydropyrazole systems as efficient telomerase inhibitors, based on the protein structure of telomerase using LigandFit module within Discovery Studio 2.1, our group has recently reported a novel docking model. When we introduced the [1,4]oxazepine moiety in the above-mentioned ary-dihydropyrazole skeleton, the novel moiety of dropyrazolo-[1,4]oxazepine with potentially higher activity against telomerase was obtained.<sup>16</sup> Recently, there have been only a few successful hTERT inhibitors developed. BIBR1532 is one of the most promising hTERT specific active site inhibitors.<sup>17</sup> BIBR1532 is an non-nucleotidic small molecule synthetic compound that inhibits telomerase by non-competitively binding to the active site of hTERT.<sup>18,19</sup> Since there are only a very few systematic reports on the synthetic methodology and evaluation of anticancer activity of this moiety, herein, as a continuation of our research for finding novel, efficient telomerase inhibitors, we designed and synthesized a series of 2-methyl-4,5-substitutedbenzo[f]-3,3a,4,5-tetrahydro-pyrazolo[1,5-d][1,4]oxazepin-8(7H)-one derivatives.

In order to further explore detailed molecular mechanism of the synthesized compounds, inhibitive activities of hTERT and



**Scheme 1.** Synthesis of 2-methyl-substitutedbenzo-3,3a-dihydropyrazolo[1,5-d][1,4] oxazepin-8(7H)-one derivatives. Reagent and conditions: (A)  $\text{CH}_3\text{COCH}_3$ ,  $\text{NaOH}$ ,  $\text{C}_2\text{H}_5\text{OH}$ , 20–30 °C, 10 h. (B)  $\text{N}_2\text{H}_4\cdot\text{H}_2\text{O}$ ,  $\text{CH}_3\text{CH}_2\text{OH}$ , reflux, 2 h. (C) 2-Bromopropanoic acid, 4-nitrobenzenesulfonyl chloride, DMAP, reflux, 2 h. (D)  $\text{NaHCO}_3$ ,  $\text{C}_2\text{H}_5\text{OH}$ , reflux 3 h. (E) 5%  $\text{HCl}$ . R = 7,9-2Br (**4a**); R = 7-Cl (**4b**); R = 9-OMe (**4c**); R = 7- $\text{CF}_3$  (**4d**); R = 8- $\text{NO}_2$  (**4e**); R = 8-Me (**4f**); R = 9-F (**4g**); R = H (**4h**).

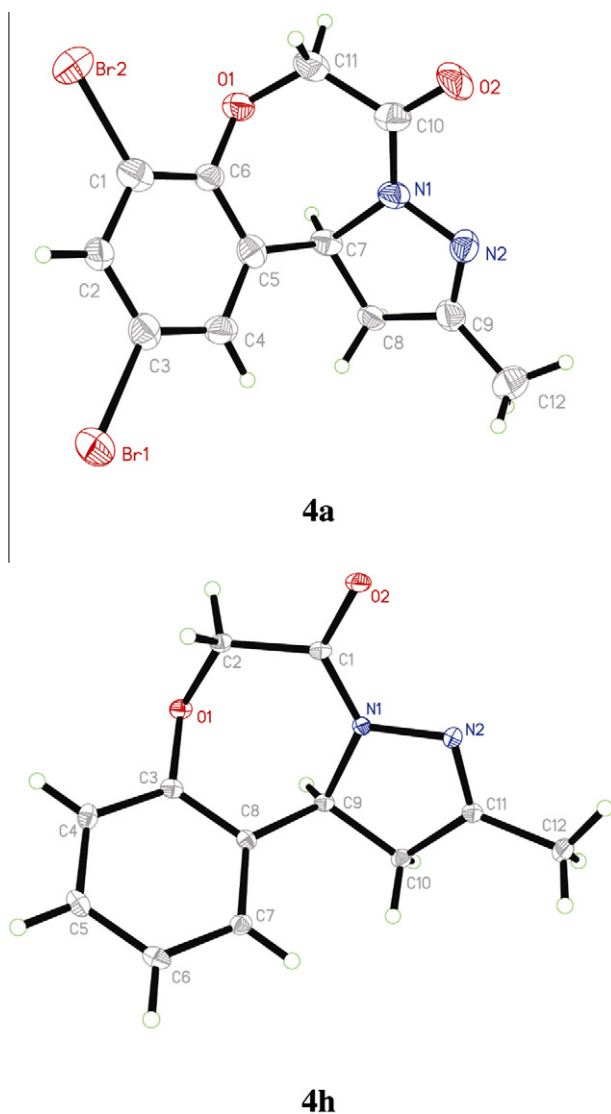


**Figure 1.** ORTEP drawing of compounds **4a** and **4h**.

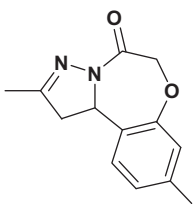
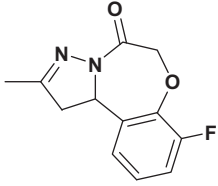
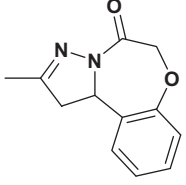
**Table 1**  
Inhibitory effects of selected compounds against telomerase

Compound	Structure	$\text{IC}_{50}^c$ ( $\mu\text{M}$ ) telomerase <sup>a</sup>
<b>4a</b>		$0.78 \pm 0.22$
<b>4b</b>		$1.71 \pm 0.51$
<b>4c</b>		$10.82 \pm 1.32$
<b>4d</b>		$3.14 \pm 1.07$
<b>4e</b>		$6.60 \pm 0.73$

phospho-AKT (p-AKT) proteins were evaluated, the results showed title compounds **4a**, **4b** could inhibit the PI3K/AKT pathway.

(continued on next page)

Table 1 (continued)

Compound	Structure	IC <sub>50</sub> <sup>c</sup> (μM) telomerase <sup>a</sup>
4f		21.90 ± 2.07
4g		2.11 ± 0.87
4h		14.80 ± 1.01
Ethidium bromide <sup>b</sup>		2.39 ± 0.12

<sup>a</sup> Telomerase supercoiling activity.<sup>b</sup> Ethidium bromide is reported as a control. The inhibition constant of ethidium toward telomerase has been reported previously.<sup>c</sup> 1 μM = 10<sup>−6</sup> mol/L.

The synthesis of compound **1** (Scheme 1) started from substituted salicylaldehyde and catalyzed by NaOH at 20–30 °C was added acetone. Compound **2** was prepared according to a previously published report.<sup>20</sup> Using catalysts 4-nitrobenzenesulfonylchloride and DMAP, proved to be an efficient alternative for the synthesis of title compound **3**. The general synthetic procedure process and spectral data of compound **4** can be found in the supporting information.<sup>21</sup>

The structures of compounds **4a**, **4h** were determined by X-ray crystallography. Crystal data of **4a**: Colorless crystals, yield, 70%; mp 177–178 °C; C<sub>12</sub> H<sub>10</sub> Br<sub>2</sub> N<sub>2</sub> O<sub>2</sub>, *M* = 374.04, Monoclinic, space group *C2/c*; *a* = 37.69(3), *b* = 9.820(9), *c* = 14.002(12) (Å);  $\alpha$  = 90,  $\beta$  = 99.851(9),  $\gamma$  = 90 (°), *V* = 5107(8) nm<sup>3</sup>, *T* = 293(2) K, *Z* = 16, *D<sub>c</sub>* = 1.946 g/cm<sup>3</sup>, *F*(000) = 2912, Reflections collected/unique = 12579/4565, Data/restraints/parameters = 4565/36/327, Goodness of fit on *F*<sup>2</sup> = 1.010, Fine, *R*<sub>1</sub> = 0.0976, *wR*(*F*<sup>2</sup>) = 0.2461. **4h**: Colorless crystals, yield, 87%; mp 168–169 °C; C<sub>12</sub> H<sub>12</sub> N<sub>2</sub> O<sub>2</sub>, *M* = 216.24, Orthorhombic, space group *Pbca*; *a* = 7.9121(2), *b* = 14.6270(4), *c* = 17.7344(5) (Å);  $\alpha$  = 90,  $\beta$  = 90,  $\gamma$  = 90 (°),

*V* = 2052.42(9) nm<sup>3</sup>, *T* = 293(2) K, *Z* = 8, *D<sub>c</sub>* = 1.400 g/cm<sup>3</sup>, *F*(000) = 912, Reflections collected/unique = 5429/2020, Data/restraints/parameters = 2020/0/146, Goodness of fit on *F*<sup>2</sup> = 1.080, Fine, *R*<sub>1</sub> = 0.0427, *wR*(*F*<sup>2</sup>) = 0.0900.

The molecular structures of compounds **4a**, **4h** were shown in Figure 1. Crystallographic data (excluding structure factors) for the structure had been deposited with the Cambridge Crystallographic Data Center as supplementary publication No. CCDC-887779, 899791.<sup>23</sup>

Some purified title compounds were assayed for telomerase inhibition,<sup>25</sup> using a MGC-803 cell extract, also included the activity of reference compound ethidium bromide.<sup>26</sup> The results were summarized in Table 1. The results suggested some compounds showed strong inhibitory activity with telomerase. Especially compounds **4a**, **4b** and **4g** with IC<sub>50</sub> values of 0.78 ± 0.22, 1.71 ± 0.51 and 2.11 ± 0.87 μM, respectively, which were even better than that of the ethidium bromide. From the data presented in Table 1, it can be concluded that halophenyl structure show higher inhibitory activity than any other structure, this pointed out the direction for us to further optimize the structures of 2-substituted-4,5-substitutedbenzo[*f*]-3,3a,4,5-tetrahydro-pyrazolo[1,5-*d*][1,4]oxazepin-8(7*H*)-one derivatives as potential telomerase inhibitors.

In order to examine whether some titled compounds change the expression of TERT, we performed western blot assays.<sup>27</sup> As shown in Figure 2, compared with adjacent control group, TERT protein was expressed at lower level in MGC-803 cells, which were treated with compounds **4a**, **4b**, **4c**, **4d**, **4f** and **4g**, respectively. The result suggested that telomerase activity was significantly down-regulated within 48 h when the cells exposed to compounds **4a**, **4b**.

In summary, based on finding novel, efficient telomerase inhibitors, we designed and synthesized some novel 2-methyl-4,5-substitutedbenzo[*f*]-3,3a,4,5-tetrahydro-pyrazolo[1,5-*d*][1,4]oxazepin-8(7*H*)-one derivatives as potential telomerase inhibitors, followed by chemical synthesis and biological evaluated for them. Among them, **4a** and **4h** were determined by X-ray. In order to examine whether some titled compounds change the expression of TERT, western blot assays showed that compounds **4a** and **4b** could inhibit the expression of Cyclin D1, TERT, phospho-AKT and the PI3K/AKT pathway. These results are of help in the rational design of more efficient telomerase inhibitors for chemoprevention and chemotherapy in further.

## Acknowledgments

The authors wish to thank the National Natural Science Foundation of China (No. 21172048, 21272008), China Postdoctoral Science Foundation funded project (2012M511948) and the Research Foundation of Doctor, Anhui Medical University (XJ201120).

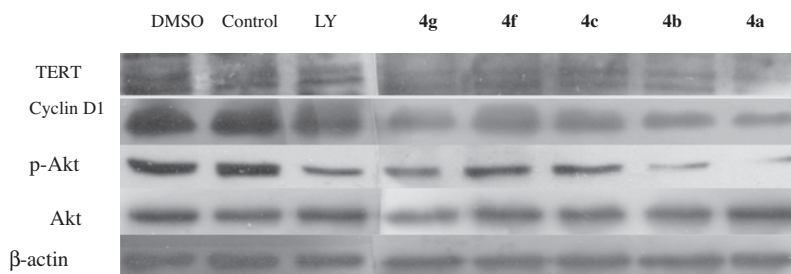


Figure 2. Western blot analyses of MGC-803 cells lysates was performed for Cyclin D1, TERT, phospho-AKT and total AKT after 48 h of incubation. β-actin served as loading control. LY294002 (25 μM) is the classic inhibitor of PI3 K/AKT pathway and DMSO was employed as negative control.

## References and notes

- Wright, W. E.; Shay, J. W. *Curr. Opin. Genet. Dev.* **2001**, *11*, 98.
- Bodnar, A. G.; Ouellette, M.; Frolakis, M.; Holt, S. E.; Chiu, C. P.; Morin, G. B.; Harley, C. B.; Shay, J. W.; Lichtsteiner, S.; Wright, W. E. *Science* **1998**, *279*, 349.
- Andrew, J. G.; Anthony, P. S.; Emmanuel, S. *Nature* **2008**, *455*, 633.
- Stewart, S. A.; Bertuch, A. A. *Cancer Res.* **2010**, *70*, 7365.
- Park, Y. P.; Kim, K. D.; Kang, S. H.; Yoon, Y.; Park, J. W.; Kim, J. W.; Lee, H. G. *Korean J. Lab. Med.* **2008**, *28*, 430.
- Hennessey, B. T.; Smith, D. L.; Ram, P. T.; Lu, Y.; Mills, G. B. *Nat. Rev. Drug Disc.* **2005**, *4*, 988.
- Robl, J. A.; Simpkins, L. M.; Asaad, M. M. *Bioorg. Med. Chem. Lett.* **2000**, *10*, 257.
- Murakami, Y.; Hara, H.; Okada, T.; Hashizume, H.; Kii, M. *J. Med. Chem.* **1999**, *42*, 2621.
- Zhang, P.; Kern, J. C.; Terefenko, E. A.; Fensome, A.; Unwalla, R.; Zhang, Z.; Cohen, J.; Berrodin, T. J.; Yudit, M. R.; Winneker, R. C.; Wrobel, J. *Bioorg. Med. Chem. Lett.* **2008**, *16*, 6589.
- Murray, P. J.; Kranz, M.; Ladlow, M.; Taylor, S.; Berst, F.; Holmes, A. B.; Keavey, K. N.; Jaxa-Chamiec, A.; Seale, P. W.; Stead, P.; Upton, R. J.; Croft, S. L.; Clegg, W.; Elsegood, M. R. *Bioorg. Med. Chem. Lett.* **2001**, *11*, 773.
- Bong, D. T.; Clark, T. D.; Granja, J. R.; Ghadiri, M. R. *Angew. Chem., Int. Ed.* **2001**, *40*, 988.
- (a) Renneberg, D.; Dervan, P. B. *J. Am. Chem. Soc.* **2003**, *125*, 5707; (b) Deng, J.; Zhao, S.; Miao, Z. *Nat. Prod. Lett.* **1993**, *2*, 283.
- Liu, X. H.; Ruan, B. F.; Li, J.; Song, B. A.; Zhu, H. L.; Bhadury, P. S.; Zhao, J. *Mini-Rev. Med. Chem.* **2011**, *11*, 771.
- Liu, X. H.; Ruan, B. F.; Liu, J. X.; Song, B. A.; Jing, L. H.; Li, J.; Yang, Y.; Zhu, H. L.; Qi, X. B. *Bioorg. Med. Chem. Lett.* **2011**, *21*, 2916.
- Liu, X. H.; Liu, H. F.; Chen, J.; Yang, Y.; Song, B. A.; Bai, L. S.; Liu, J. X.; Zhu, H. L.; Qi, X. B. *Bioorg. Med. Chem. Lett.* **2010**, *20*, 5705.
- Liu, X. H.; Li, J.; Shi, J. B.; Song, B. A.; Qi, X. B. *Eur. J. Med. Chem.* **2012**, *51*, 294.
- Damm, K.; Hemmann, U.; Garin-Chesa, P. *EMBO J.* **2001**, *20*, 6958.
- Pascolo, E.; Wenz, C.; Lingner, J.; Haul, N.; Priepke, H.; Kauffmann, I. *J. Biol. Chem.* **2002**, *277*, 15566.
- El-Daly, H.; Kull, M.; Zimmermann, S.; Pantic, M.; Waller, C. F.; Martens, U. M. *Blood* **2005**, *105*, 1742.
- Liu, X. H.; Zhu, J.; Zhou, A. N.; Song, B. A.; Zhu, H. L.; Bai, L. S.; Bhadury, P. S.; Pan, C. X. *Bioorg. Med. Chem. Lett.* **2009**, *17*, 1207.
- General synthetic procedure process for compound **4**: To a C<sub>2</sub>H<sub>5</sub>OH (20 ml) solution of NaHCO<sub>3</sub> (10 mmol) was added 2-bromo-1-(5-(2-hydroxy-substitutedphenyl)-3-methyl-4,5-dihydropyrazol-1-yl)ethanone **3** (10 mmol), then the reaction mixture was refluxed for 3 h. The mixture was allowed to cool to room temperature and 30 ml water was added, adjusted pH to 7 with 5% HCl solution, allowed to stand at 0 °C over night. The product was collected by filtration and the crude residue was purified by chromatography on SiO<sub>2</sub> (acetone/petroleum, v:v = 2:1) to give title compound **4** (Scheme 1) as colorless solids.<sup>22</sup>
- 4a**: Colorless crystals, yield, 70%; mp 177–178 °C; <sup>1</sup>H NMR (400 MHz, CDCl<sub>3</sub>)  $\delta$  (ppm): 2.06 (s, 3H, -CH<sub>3</sub>), 3.32 (dd, 1H, *J*<sub>1</sub> = 4.0 Hz, *J*<sub>2</sub> = 8.0 Hz, pyrazole 4-H<sub>a</sub>), 3.61 (dd, 1H, *J*<sub>1</sub> = 8.0 Hz, *J*<sub>2</sub> = 16.0 Hz, pyrazole 4-H<sub>b</sub>), 4.29 (d, 1H, *J* = 16.0 Hz, oxazepane 2-H<sub>a</sub>), 5.00 (d, 1H, *J* = 16.0 Hz, oxazepane 2-H<sub>b</sub>), 5.84 (dd, 1H, *J*<sub>1</sub> = 8.0 Hz, *J*<sub>2</sub> = 12.0 Hz, pyrazole 5-H), 7.67 (d, 1H, *J* = 1.6 Hz), 7.93 (d, 1H, *J* = 2.4 Hz). Anal. Calcd for C<sub>12</sub>H<sub>10</sub>BrN<sub>2</sub>O<sub>2</sub>: C, 38.53; H, 2.69; N, 7.49. Found: C, 38.19; H, 3.00; N, 7.25.
- 4b**: Colorless crystals, yield, 60%; mp 182–183 °C; <sup>1</sup>H NMR (400 MHz, CDCl<sub>3</sub>)  $\delta$  (ppm): 2.00 (s, 3H, -CH<sub>3</sub>), 3.37 (dd, 1H, *J*<sub>1</sub> = 4.0 Hz, *J*<sub>2</sub> = 8.0 Hz, pyrazole 4-H<sub>a</sub>), 3.69 (dd, 1H, *J*<sub>1</sub> = 8.0 Hz, *J*<sub>2</sub> = 16.0 Hz, pyrazole 4-H<sub>b</sub>), 4.21 (d, 1H, *J* = 16.0 Hz, oxazepane 2-H<sub>a</sub>), 5.08 (d, 1H, *J* = 16.0 Hz, oxazepane 2-H<sub>b</sub>), 5.77 (dd, 1H, *J*<sub>1</sub> = 8.0 Hz, *J*<sub>2</sub> = 12.0 Hz, pyrazole 5-H), 7.21–7.40 (m, 3H, ArH's). Anal. Calcd for C<sub>12</sub>H<sub>11</sub>ClN<sub>2</sub>O<sub>2</sub>: C, 57.49; H, 4.42; N, 11.17. Found: C, 57.65; H, 4.71; N, 11.03.
- 4c**: Colorless crystals, yield, 71%; mp 166–167 °C; <sup>1</sup>H NMR (400 MHz, CDCl<sub>3</sub>)  $\delta$  (ppm): 2.11 (s, 3H, -CH<sub>3</sub>), 3.42 (dd, 1H, *J*<sub>1</sub> = 4.0 Hz, *J*<sub>2</sub> = 8.0 Hz, pyrazole 4-H<sub>a</sub>), 3.75 (dd, 1H, *J*<sub>1</sub> = 8.0 Hz, *J*<sub>2</sub> = 16.0 Hz, pyrazole 4-H<sub>b</sub>), 3.83 (s, 3H, -OCH<sub>3</sub>), 4.27 (d, 1H, *J* = 16.0 Hz, oxazepane 2-H<sub>a</sub>), 5.02 (d, 1H, *J* = 16.0 Hz, oxazepane 2-H<sub>b</sub>), 5.64 (dd, 1H, *J*<sub>1</sub> = 8.0 Hz, *J*<sub>2</sub> = 12.0 Hz, pyrazole 5-H), 6.88–7.19 (m, 3H). Anal. Calcd for C<sub>13</sub>H<sub>14</sub>N<sub>2</sub>O<sub>3</sub>: C, 63.40; H, 5.73; N, 11.38. Found: C, 63.18; H, 6.02; N, 11.21.
- 4d**: Colorless crystals, yield, 60%; mp 170–172 °C; <sup>1</sup>H NMR (400 MHz, CDCl<sub>3</sub>)  $\delta$  (ppm): 2.02 (s, 3H, -CH<sub>3</sub>), 3.33 (dd, 1H, *J*<sub>1</sub> = 4.0 Hz, *J*<sub>2</sub> = 8.0 Hz, pyrazole 4-H<sub>a</sub>), 3.65 (dd, 1H, *J*<sub>1</sub> = 8.0 Hz, *J*<sub>2</sub> = 16.0 Hz, pyrazole 4-H<sub>b</sub>), 4.15 (d, 1H, *J* = 16.0 Hz, oxazepane 2-H<sub>a</sub>), 4.97 (d, 1H, *J* = 16.0 Hz, oxazepane 2-H<sub>b</sub>), 5.65 (dd, 1H, *J*<sub>1</sub> = 8.0 Hz, *J*<sub>2</sub> = 12.0 Hz, pyrazole 5-H), 7.08–7.35 (m, 3H). Anal. Calcd for C<sub>13</sub>H<sub>11</sub>F<sub>3</sub>N<sub>2</sub>O<sub>2</sub>: C, 54.93; H, 3.90; N, 9.86. Found: C, 55.15; H, 4.04; N, 10.10.
- 4e**: Colorless crystals, yield, 81%; mp 182–183 °C; <sup>1</sup>H NMR (400 MHz, CDCl<sub>3</sub>)  $\delta$  (ppm): 2.11 (s, 3H, -CH<sub>3</sub>), 3.39 (dd, 1H, *J*<sub>1</sub> = 4.0 Hz, *J*<sub>2</sub> = 8.0 Hz, pyrazole 4-H<sub>a</sub>), 3.71 (dd, 1H, *J*<sub>1</sub> = 8.0 Hz, *J*<sub>2</sub> = 16.0 Hz, pyrazole 4-H<sub>b</sub>), 4.19 (d, 1H, *J* = 16.0 Hz, oxazepane 2-H<sub>a</sub>), 5.04 (d, 1H, *J* = 16.0 Hz, oxazepane 2-H<sub>b</sub>), 5.77 (dd, 1H, *J*<sub>1</sub> = 8.0 Hz, *J*<sub>2</sub> = 12.0 Hz, pyrazole 5-H), 7.45–7.94 (m, 3H). Anal. Calcd for C<sub>12</sub>H<sub>11</sub>N<sub>3</sub>O<sub>4</sub>: C, 55.17; H, 4.24; N, 16.09. Found: C, 55.42; H, 4.53; N, 15.87.
- 4f**: Colorless crystals, yield, 72%; mp 164–165 °C; <sup>1</sup>H NMR (400 MHz, CDCl<sub>3</sub>)  $\delta$  (ppm): 2.11 (s, 3H, -CH<sub>3</sub>), 2.49 (s, 3H, -CH<sub>3</sub>), 3.30 (dd, 1H, *J*<sub>1</sub> = 4.0 Hz, *J*<sub>2</sub> = 8.0 Hz, pyrazole 4-H<sub>a</sub>), 3.62 (dd, 1H, *J*<sub>1</sub> = 8.0 Hz, *J*<sub>2</sub> = 16.0 Hz, pyrazole 4-H<sub>b</sub>), 4.17 (d, 1H, *J* = 16.0 Hz, oxazepane 2-H<sub>a</sub>), 5.00 (d, 1H, *J* = 16.0 Hz, oxazepane 2-H<sub>b</sub>), 5.63 (dd, 1H, *J*<sub>1</sub> = 8.0 Hz, *J*<sub>2</sub> = 12.0 Hz, pyrazole 5-H), 6.75–7.19 (m, 3H). Anal. Calcd for C<sub>13</sub>H<sub>14</sub>N<sub>2</sub>O<sub>2</sub>: C, 67.81; H, 6.13; N, 12.17. Found: C, 68.03; H, 5.87; N, 12.45.
- 4g**: Colorless crystals, yield, 74%; mp 175–177 °C; <sup>1</sup>H NMR (400 MHz, CDCl<sub>3</sub>)  $\delta$  (ppm): 2.17 (s, 3H, -CH<sub>3</sub>), 3.35 (dd, 1H, *J*<sub>1</sub> = 4.0 Hz, *J*<sub>2</sub> = 8.0 Hz, pyrazole 4-H<sub>a</sub>), 3.65 (dd, 1H, *J*<sub>1</sub> = 8.0 Hz, *J*<sub>2</sub> = 16.0 Hz, pyrazole 4-H<sub>b</sub>), 4.12 (d, 1H, *J* = 16.0 Hz, oxazepane 2-H<sub>a</sub>), 5.05 (d, 1H, *J* = 16.0 Hz, oxazepane 2-H<sub>b</sub>), 5.72 (dd, 1H, *J*<sub>1</sub> = 8.0 Hz, *J*<sub>2</sub> = 12.0 Hz, pyrazole 5-H), 6.89–7.01 (m, 3H). Anal. Calcd for C<sub>12</sub>H<sub>11</sub>FN<sub>2</sub>O<sub>2</sub>: C, 61.53; H, 4.73; N, 11.96. Found: C, 61.25; H, 4.99; N, 12.10.
- 4h**: Colorless crystals, yield, 87%; mp 168–169 °C; <sup>1</sup>H NMR (400 MHz, CDCl<sub>3</sub>)  $\delta$  (ppm): 2.05 (s, 3H, -CH<sub>3</sub>), 3.32 (dd, 1H, *J*<sub>1</sub> = 4.0 Hz, *J*<sub>2</sub> = 8.0 Hz, pyrazole 4-H<sub>a</sub>), 3.60 (dd, 1H, *J*<sub>1</sub> = 8.0 Hz, *J*<sub>2</sub> = 16.0 Hz, pyrazole 4-H<sub>b</sub>), 4.17 (d, 1H, *J* = 16.0 Hz, oxazepane 2-H<sub>a</sub>), 5.00 (d, 1H, *J* = 16.0 Hz, oxazepane 2-H<sub>b</sub>), 5.63 (dd, 1H, *J*<sub>1</sub> = 8.0 Hz, *J*<sub>2</sub> = 12.0 Hz, pyrazole 5-H), 6.84–7.00 (m, 4H). Anal. Calcd for: C<sub>12</sub>H<sub>12</sub>N<sub>2</sub>O<sub>2</sub>: C, 66.65; H, 5.59; N, 12.96. Found: C, 66.70; H, 5.47; N, 13.18.
- The reactions were monitored by thin layer chromatography (TLC) on Merck pre-coated silica GF254 plates. Melting points (uncorrected) were determined on a XTAMP apparatus (Taike Corp., Beijing, China). <sup>1</sup>H NMR spectra were collected on PX400 spectrometer at room temperature with TMS and solvent signals allotted as internal standards. Chemical shifts are reported in ppm ( $\delta$ ). Elemental analyses were performed on a CHN-O-Rapid instrument, and were within  $\pm 0.4\%$  of the theoretical values.
- Crystallographic studies**: X-ray single-crystal diffraction data for compounds **4a**, **4h** (a sample of size 0.26  $\times$  0.23  $\times$  0.22 and 0.31  $\times$  0.27  $\times$  0.21 mm<sup>3</sup>) was collected on a Bruker SMART APEX CCD diffractometer at 296(2) K using MoK $\alpha$  radiation ( $\lambda$  = 0.71073 Å) by the  $\omega$  scan mode. The program SAINT was used for integration of the diffraction profiles. The structure was solved by direct methods using the SHELXS program of the SHELXTL package and refined by full-matrix least-squares methods with SHELXL.<sup>24</sup> The corrections for LP factors were applied. All non-hydrogen atoms of compounds **4a**, **4h** were refined with anisotropic thermal parameters. All hydrogen atoms were generated theoretically onto the parent atoms and refined isotropically with fixed thermal factors.
- Sheldrick, G. M. SHELXTL-97, Program for Crystal Structure Solution and Refinement; University of Göttingen: Göttingen, Germany, 1997.
- Kim, N. W.; Piatyszek, M. A.; Prowse, K. R.; Harley, C. B.; West, M. D.; Ho, P. L.; Coviello, G. M.; Wright, W. E.; Weinrich, S. L.; Shay, J. W. *Science* **2011**, *1994*, 266.
- Telomerase activity assay**: Compounds **4** were tested in a search for small molecule inhibitors of telomerase activity by using the TRAP-PCR-ELISA assay. In detail, the MGC-803 cells were firstly maintained in DMEM medium (GIBCO, New York, USA) supplemented with 10% fetal bovine serum (GIBCO, New York, USA), streptomycin (0.1 mg/mL) and penicillin (100 IU/mL) at 37 °C in a humidified atmosphere containing 5% CO<sub>2</sub>. After trypsinization, 5  $\times$  10<sup>4</sup> cultured cells in logarithmic growth were seeded into T25 flasks (Corning, New York, USA) and cultured to allow to adherence. The cells were then incubated with Staurosporine (Santa Cruz, Santa Cruz, USA) and the drugs with a series of concentration as 60, 20, 6.67, 2.22, 0.74, 0.25 and 0.0821 g/mL, respectively. After 24 h treatment, the cells were harvested by cell scraper orderly following by washed once with PBS. The cells were lysed in 150  $\mu$ L RIPA cell lysis buffer (Santa Cruz, Santa Cruz, USA), and incubated on ice for 30 min. The cellular supernatants were obtained via centrifugation at 12,000 g for 20 min at 4 °C and stored at -80 °C. The TRAP-PCR-ELISA assay was performed using a telomerase detection kit (Roche, Basel, Switzerland) according to the manufacturer's protocol. In brief, 2  $\mu$ L of cell extracts were mixed with 48  $\mu$ L TRAP reaction mixtures. PCR was then initiated at 94 °C, 120 s for predenaturation and performed using 35 cycles each consisting of 94 °C for 30 s, 50 °C for 30 s, 72 °C for 90 s. Then 20  $\mu$ L of PCR products were hybridized to a digoxigenin (DIG)-labeled telomeric repeat specific detection probe. And the PCR products were immobilized via the biotin-labeled primer to a streptavidin-coated microtiter plate subsequently. The immobilized DNA fragment were detected with a peroxidase-conjugated anti-DIG antibody and visualized following addition of the stop reagent. The microtitre plate was assessed on TECAN Infinite M200 microplate reader (Mannedorf, Switzerland) at a wavelength of 490 nm, and the final value were presented as mean  $\pm$  SD.
- Western blotting**: Mouse anti-TERT monoclonal antibody and rabbit anti-Cyclin D1 monoclonal antibody were purchased from Abcam (Cambridge, UK) and Vector (Switzerland), respectively. AKT and phospho-AKT antibodies were purchased from Cell Signaling (Beverly, MA, USA). Secondary antibodies for goat anti-rabbit immunoglobulin (Ig) G horse radish peroxidase (HRP), goat anti-mouse IgG HRP was purchased from Santa Cruz Biotechnology (California, USA).  $\beta$ -actin antibody was obtained from Santa Cruz Biotechnology (California, USA). Dimethyl sulfoxide (DMSO) was purchased from Sigma Inc. (St. Louis, MO, USA). Human MGC-803 cells were lysed with RIPA lysis buffer (Beyotime, China). Whole extracts were prepared, and protein concentration was detected using a BCA protein assay kit (Beyotime, China). Total protein (30 or 50 mg) from samples were separated by SDS-PAGE and blotted onto a PVDF membrane (Millipore Corp, Billerica, MA, USA). After blockade of nonspecific protein binding, nitrocellulose blots were incubated for 1 h with primary antibodies diluted in TBS/Tween-20 (0.075%) containing 3% Marvel. Mouse monoclonal antibody recognizing TERT (Abcam, UK) was used 1:500 as was anti- $\beta$ -actin (Santa Cruz, USA), rabbit monoclonal antibody recognizing Cyclin D1 (vector, Switzerland) was used 1:500, rabbit monoclonal anti phospho-AKT (Cell Signaling, USA) was diluted 1:500 as was anti-AKT (Cell Signaling, USA). Horseradish peroxidase conjugated anti-mouse and anti-rabbit antibodies were used as secondary antibodies correspondingly. After extensive washing in TBS/Tween-20, the blots were processed with distilled water for detection of antigen using the enhanced chemiluminescence system. Proteins were visualized with ECL-chemiluminescent kit (ECL-plus, Thermo Scientific).